Trimuon and dimuon events produced by 10.5-GeV/c μ^- on lead

J. LeBritton, D. McCal,* A. Melissinos, W. Metcalf,† and M. Miller‡
Department of Physics and Astronomy, University of Rochester, Rochester, New York 14627

J. Alspector,§ S. Borenstein,‖ G. Kalbfleisch,¶ J. Scharenguivel, and R. Strand
Brookhaven National Laboratory, Upton, New York 11973

A. Abashian
National Science Foundation, Washington, D.C. 20550

(Received 16 June 1980)

We report on the production of 158 trimuon and 637 dimuon events by 10.5-GeV/c muons incident on lead. The sensitivity of the experiment was typically 1 event per picobarn per nucleon. It is shown that the majority of the trimuon events are due to QED trident production. We present differential and total cross sections for this process and establish that muons obey Fermi-Dirac statistics at a confidence level of 8 standard deviations. Approximately 10% of the trimuons are due to other processes, most probably diffraction of the virtual photon. Upper limits on the production of particles with a three-muon decay mode and on inelastic virtual-photon Compton scattering are obtained. The dimuon events can be accounted for by tridents where one of the muons lies outside the acceptance of the apparatus and by the production of π and K mesons which subsequently decay into a muon. Upper limits on *prompt* single-muon production are given.

I. INTRODUCTION

As part of a general experimental investigation of muon interactions on heavy nuclei we report here on events with final states containing two and three muons

$$\begin{aligned} &\mu^- + \mathrm{Pb} \to \mu^-\mu^-\mu^+ + \mathrm{Pb}\,, \\ &\mu^- + \mathrm{Pb} \to \mu^-\mu^-\mu^+ + X\,, \\ &\mu^- + \mathrm{Pb} \to \mu^-\mu^\pm + X\,. \end{aligned} \tag{1}$$

Preliminary results from this data have been given in a previous publication.[1] The experiment was performed at the Brookhaven National Laboratory Alternating Gradient Synchrotron (AGS) with a muon beam of momentum 10.5 ± 1.3 GeV/c. The sample of dimuon and trimuon events was obtained with the beam incident on a 13-in. lead-glass target. Final-state muons were detected with a wide-angle muon spectrometer equipped with multiwire proportional chambers (MWPC's). A total of 158 trimuon and 637 dimuon events were observed.

In this experiment the trimuon yield is dominated by the coherent production of muon pairs in the field of the target nucleus, or muon tridents. The four Feynman diagrams for this process are shown in Fig. 1. Graphs 1(a) and 1(b) represent pair production by a spacelike ($q^2 < 0$) virtual photon, while in graphs 1(c) and 1(d) the photon propagator between muons is timelike ($q^2 > 0$). These reactions are predominant when the photon exchanged with the nucleus is at very low q^2 ($|q_N^2| < 0.01$ GeV^2), hence the cross section for production off nuclear targets is proportional to Z^2, moderated by the nuclear form factor. The trident matrix elements have been calculated by Brodsky and Ting,[2] and reevaluated by several authors[2] with excellent agreement. For our calculations we have used the results of Ref. 1 and evaluated the cross sections with a Monte Carlo integration program written by Tannenbaum.[3]

The muon-trident process is unique in that it is the only one studied to date in which two identical direct muons are present in the final state. Hence, in addition to providing a test of QED, the observation of tridents can be used to test muon statis-

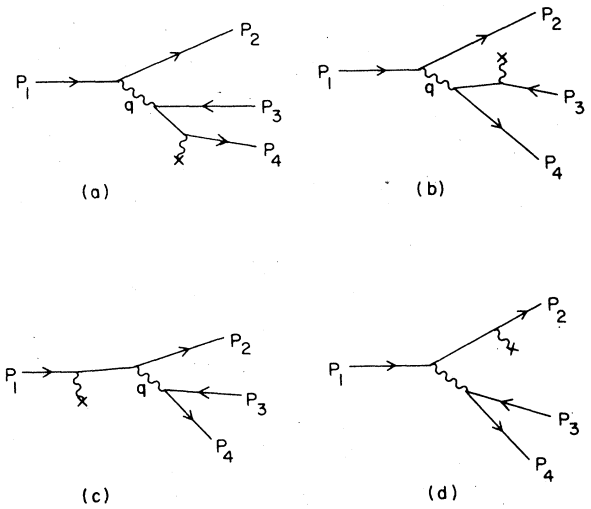

FIG. 1. The four Bethe-Heitler Feynman diagrams for the muon trident process. The "scattering" graphs (a) and (b) are produced by a spacelike virtual photon. In the "dissociation" graphs (c) and (d) the incident muon radiates a timelike virtual photon.

tics (i.e., the antisymmetry of the muon wave function). An electron-trident experiment was performed by Criegee *et al.*[4] and muon tridents have been observed with cosmic-ray muons,[5] but it was not until the experiment of Russell *et al.*[6] that the cross section was reliably measured and muons were first shown to obey Fermi-Dirac statistics.

The theoretical differential cross section (in the first Born approximation) as a function of the effective mass $M_{\mu^-\mu^-}$ of the two like-sign muons is shown in Fig. 2 for a lead target at 12 and 200 GeV. We note the following features: (a) The trident cross section increases with incident energy ($\sigma_{tot}=0.8$ μb/Pb nucleus at 12 GeV, $\sigma_{tot}=12.1$ μb/Pb nucleus at 200 GeV). (b) The coherence of the trident process off nuclei induces a large difference (a factor of ~4000) between lead and proton cross sections. However, at high energies and large effective masses ($M_{\mu\mu} \geq 10$ GeV/c^2) the incoherent scattering off individual nucleons starts to dominate over the coherent process due to the increased momentum transfer to the target.[7] (c) At very low effective mass $M_{\mu^-\mu^-}$ the wave functions of the two identical muons overlap significantly (small opening angle, similar momenta). Thus, for Fermi-Dirac particles the interference of normal and exchange amplitudes (the diagrams of Fig. 1 with P_2 and P_4 interchanged) depresses the cross section in this kinematic region. This effect is the clearest signature of antisymmetry under interchange of identical muons.[3]

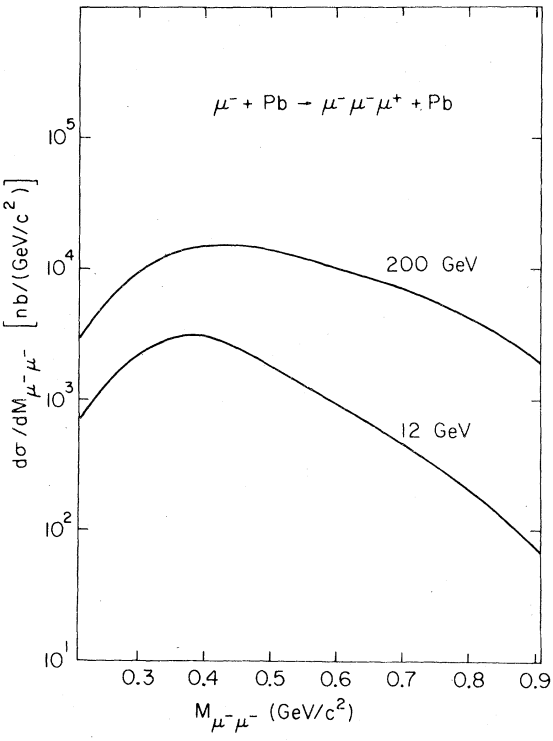

FIG. 2. QED prediction for $d\sigma/dM$, the differential cross section in the effective mass of the two beamlike muons for a lead target at 12 and 200 GeV.

In addition to the graphs shown in Fig. 1, other trimuon processes can contribute as shown in Figs. 3(a)–3(d). Graph 3(a) follows from the vector-dominance model[8] and has been extensively studied in electroproduction processes.[9] We refer to it as "strong diffraction" and there is evidence that at high energies this process becomes dominant.[10] Graph 3(b) is referred to as "inelastic virtual-photon Compton scattering" and may occur on a constituent of the nucleon. Its contribution in comparison to the trident process is expected to be small[11] because of the known low level of two-photon-exchange effects in inclusive muon-nucleus scattering.[12] On the other hand, measurements of photoproduction of muon pairs off beryllium[13] and inelastic photon-proton scattering[14] indicate that QED and the Compton process cannot account for the total cross section in the deep-inelastic region. Finally, it is possible that a pair of short-lived particles is produced, one or both of which decay into muons as depicted in Fig. 3(c). Charm or (known) heavy-lepton production is irrelevant to the present experiment since it is below $D\bar{D}$ and $\tau\bar{\tau}$ threshold ($W_{max} \approx 4.5$ GeV, where W is the photon-nucleon c.m. energy). In principle one could also consider production of trimuons through the weak interaction but such processes are completely masked by electromagnetic effects.

We have also searched for any possible enhancements in the three-muon effective-mass spectrum

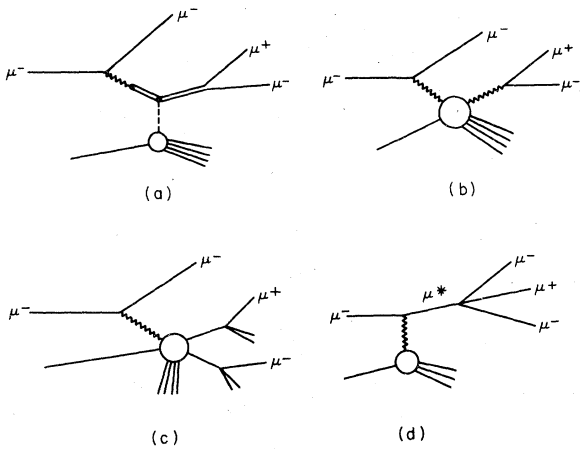

FIG. 3. Possible non-Bethe-Heitler trimuon processes as described in the text. (a) Diffractive pair production. (b) Inelastic virtual-photon Compton scattering. (c) Production of short-lived particles with muonic decay modes. (d) Primakoff effect $\mu \rightarrow \mu^* \rightarrow 3\mu$.

Such an enhancement could arise if the muon had excited states that decay into three muons and that could be reached from the ground state through an electric dipole transition [Primakoff effect,[15] Fig. 3(d)]. It has also been proposed by Pati and Salam[16] that a quark may dissociate into three muons. We have observed no evidence for such decays.

Single-prompt-muon production with muon beams has generated considerable interest recently as possible evidence for charm production.[17] In light of this, our large yield of dimuon events requires a careful interpretation. Two backgrounds can significantly contribute to a dimuon signal. Firstly, one must consider trident production in which one final-state muon, due to its low energy, falls outside the range of the experimental acceptance. Secondly, dimuons can result through the muon-induced production of π and K mesons which decay in flight into a muon. A detailed Monte Carlo calculation of these two processes produces good agreement with the data in terms of distributions, numbers of events, and charge ratios. We are thus able to impose limits on single μ^+ and μ^- production with μ^- beams at AGS energies.

In Sec. II we discuss the apparatus, event acquisition, and the data-reduction procedure leading to the trimuon and dimuon samples. In Sec. III we discuss the trimuon data with emphasis on the trident contribution. We compare the predicted and observed total cross section and present experimentally obtained differential cross sections for trident production in the effective masses, and in the energy and transverse momentum of the produced opposite-sign muon. In addition, we show new evidence for muons obeying Fermi-Dirac statistics. Excellent agreement with the predictions of QED is found throughout. A smaller sample of trimuon events which are not characteristic of the trident process is examined. We interpret these events as the diffractive production of Fig. 3(a) and establish an upper limit on the cross section in the region of the low-mass vector mesons. We compare this with results on the electroproduction of vector mesons. The three-muon mass spectrum is presented, establishing an upper limit on the production and decay of any exotic objects which have a 3μ decay mode. Finally, we discuss a small sample of *inelastic* trimuon events which could arise, for example, from the Compton scattering process of Fig. 3(b). In Sec. IV the dimuon sample is discussed in terms of conventional processes.

II. APPARATUS AND DATA REDUCTION

The muon beam was obtained from the decay of negative pions produced by the external proton beam of the Brookhaven AGS incident on the C-1 target. Pions were absorbed in 1.2 m of carbon and 6 m of beryllium while transported to the experimental area. The original beam design is due to T. Yamanouchi[18] and was upgraded to 10.5 GeV/c by H. Brown.[19] The main parameters of the beam are given in Table I. A scintillator hodoscope consisting of 218 elements in seven planes provided trajectory and momentum information for every incident particle.

A schematic of the detector is shown in Fig. 4. It consisted of a forward spectrometer utilizing a 120-in.-wide, 36-in.-deep, and 30-in.-high dipole magnet of field strength $\int B\,dl \simeq 1$ Tm. A 6000-wire MWPC system provided particle tracking and was read out via CAMAC to a Honeywell DDP-516 computer. Three scintillator planes (labeled $S100$, $S200$, and $S300$) were used for triggering. The target consisted of 12 $\frac{17}{16}$-inch slabs of lead glass each viewed by a photomultiplier to provide information on electromagnetic showers. Two 1-in.-thick DE/DX counters were placed after the target to signal the emergence of more than one minimum-ionizing particle. The $S200$ and $S300$ counters were placed front and back of a 1.5-m iron absorber to provide muon identification. They were combined in a coincidence matrix which only accepted counter combinations directed at the magnet aperture (labeled μ). A wall of veto counters (V) covered the region around the beam entrance.

A valid beam track was defined by three beam counters (A, B, C), at least one hit in each of the seven beam hodoscopes, and no veto. A spacer circuit suppressed events where two beam particles arrived within a 20-nsec time interval. Thus

$$\text{BEAM} = (A \cdot B \cdot C) \cdot (H_1, \ldots, H_7) \cdot (\Sigma \overline{V}) \cdot \qquad (2)$$

The trigger consisted of a beam track together with one of the DE/DX counters above the two minimum-ionizing particle threshold, two or more distinct μ signals, and one or more hits in the $S100$ plane.

$$T = (\text{BEAM}) \cdot (DE/DX) \cdot (S100 \geq 1) \cdot (\mu \geq 2) . \qquad (3)$$

Counter and trigger efficiencies were continuously

TABLE I. AGS muon-beam parameters.

Mean momentum	10.5 GeV/c
Momentum spread	±1.3 GeV/c
Horizontal size (FWHM)	6.3 cm
Vertical size (FWHM)	6.6 cm
Horizontal angular spread	13 mrad
Vertical angular spread	11 mrad
Pion contamination	<0.01%

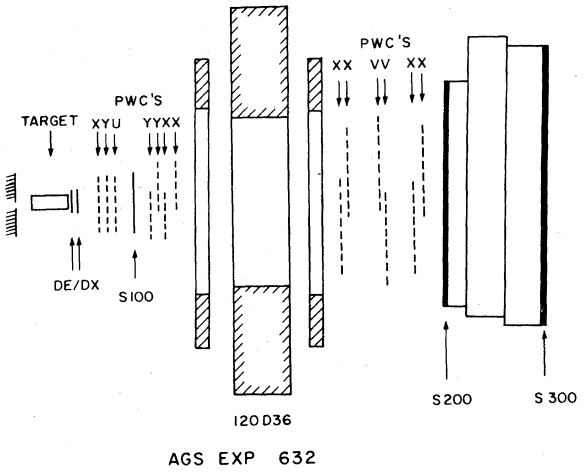

FIG. 4. Schematic of AGS experiment 632 muon spectrometer. Details are given in the text.

monitored during the experiment via a data link to the AGS on-line PDP-10 system. Pulse height and timing information for all appropriate counters were recorded.

For part of the running a 24-in. brass absorber was placed after the target to reduce muons from π and K decay. The data obtained with this configuration was useful for diagnostic purposes but is not included in the present analysis. This is because multiple-scattering in the brass impairs vertex and mass resolution and because energy loss in the absorber severely restricts the available phase space for a three-muon final state.[20]

The data presented here was obtained with an accumulated flux of 2.1×10^{10} muons incident on the lead-glass target (2.36×10^{23} Pb nuclei/cm^2). All events with three tracks, one of which was opposite in charge to the beam, were considered as trimuon candidates. All three tracks were required to be in time to within ±4 nsec in the $S100$ plane and ±6 nsec in the $S200$ and $S300$ planes. In addition, at least two tracks were required to intersect $S300$ counters that were on. Finally, it was required that the point of closest approach between the three tracks and the beam track lie within 20 cm of the target along the beam axis and inside the target transverse to the beam. This procedure produced a sample of 456 events.

In order to facilitate comparison with theory and to be certain that all three tracks were muons we accepted in the final sample only events where all three tracks had $p>1.8$ GeV/c. Furthermore, at least two of the three tracks had to be unambigously defined as muons. Ambiguity in muon identification could arise when two tracks intersected the same $S300$ counter (these counters were 18 in. wide). These cuts resulted in a sample of 158 trimuons; for 43 of these events one of the

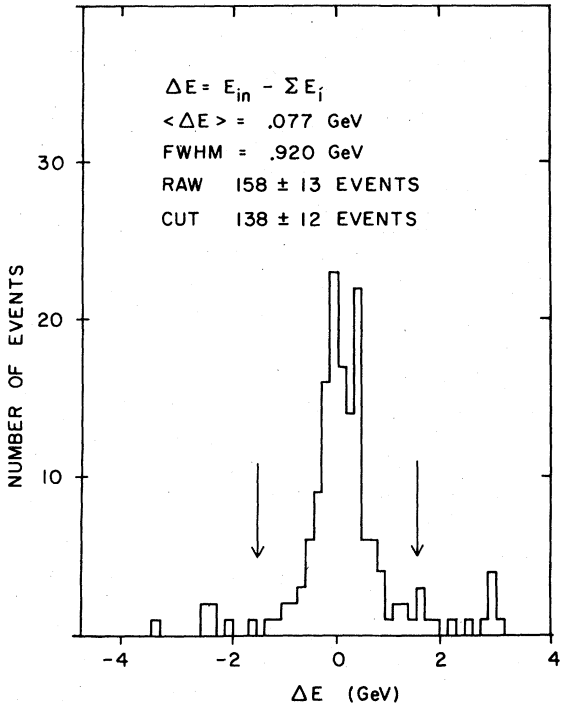

FIG. 5. The ΔE distribution for the trimuon sample. The data was cut at $|\Delta E|<1.5$ GeV as indicated by the arrows.

muons was not defined unambiguously. These 43 events were considered separately in the final analysis and their presence in the sample was found to be consistent with the Monte Carlo calculation.

In trident production, the heavy nuclear target provides momentum balance but absorbs very little energy (~50 MeV).[3] We define ΔE as the beam energy minus the sum of the energies of the final-state muons. The requirement $\Delta E\approx0$ then provides a tight constraint for identifying trident events. Each track was extrapolated to the vertex taking into account energy loss in the apparatus. A clear peak is seen in the ΔE distribution (Fig. 5) centered at $\Delta E=80$ MeV with full width at half maximum (FWHM)$=920$ MeV. The resolution in ΔE is dominated by measurement errors in the particle momentum ($\Delta p/p\approx0.015p$, p in GeV/c) and uncertainty in the position of the vertex. A cut $|\Delta E|<1.5$ GeV was imposed leaving a final sample of 138 raw trident events. In 34 of these events one muon was not defined unambiguously.

Next the data were corrected for detection efficiency by assigning an appropriate weight to each track depending on the chamber that it crossed. The efficiency of the chambers was determined for each run by observing beam tracks and was taken to be uniform over each chamber. The

overall correction for the detection of all three tracks was +24%. The background under the ΔE peak, estimated from the events outside the ΔE cut, amounted to a correction of −17%. Finally, the number of trimuon events originating from bremsstrahlung of real photons and subsequent pair production in the target was estimated using the photon distributions and conversion lengths given by Tsai[21] to be 6.1 ± 1.5. A summary of all corrections applied to the elastic trimuon sample is given in Table II, showing a final total of 137 ± 12 events.

The initial sample of 456 trimuons had the charge combination expected for pair production $(- - +)$, yet only 11 candidates were found with the wrong combination $(- + +)$. After the imposition of cuts, no "wrong-charge" events survived indicating that the trimuon background from meson decay is negligible.

For the extraction of the dimuon sample, no ΔE cut can be imposed, so it is difficult to constrain the data. The raw data were scanned for events which contained two tracks satisfying the same timing, vertexing, and momentum cuts as the trimuon sample described above. It was then required that both particles penetrate the muon filter and hit different S300 counters, ensuring absolute muon identification. This procedure produced a sample of 412 $\mu^+\mu^-$ and 216 $\mu^-\mu^-$ events. A search for $\mu^+\mu^+$ events yielded a sample of only 5 events establishing that the dimuons are almost entirely due to beam-particle interactions. The kinematic cuts imposed for the investigation of these events are described in Sec. IV below.

TABLE II. Corrections to trident sample.

Data	Number of events
Raw candidates	456
With geometry, momentum, μ-identification cuts	158
$\lvert\Delta E\rvert < 1.5$ GeV cut	138 ± 12
Corrections	
Detection and reconstruction efficiency	$+33 \pm 6$
Background subtraction	-28 ± 5
Bremsstrahlung + pair production	-6 ± 2
Total yield	137 ± 14

III. TRIMUON EVENTS

A. Elastic events; tridents

We label as "elastic" the trimuon events contained in the $\lvert\Delta E\rvert < 1.5$ GeV cut and expect that the majority will be accounted for by the trident process of Fig. 1. These graphs represent the first Born approximation and were evaluated with the Monte Carlo integration program of Ref. 3 which gave differential cross sections in angles, momenta, effective masses, and transverse momenta. Beam tracks measured in the experiment were fed to the Monte Carlo program which generated events and a weight proportional to the differential cross section. The cross section was calculated under the assumption of both Fermi-Dirac muons and muons exhibiting no exchange.[22] Since the Born series for a lead target converges slowly (in powers of $Z\alpha \approx 0.6$), a correction for the second-order term $[\sim(Z\alpha)^4]$ was included. It was estimated to be −12% based on the two-photon exchange amplitudes for muon pair photoproduction calculated by Bethe and Maximon[23] and Brodsky and Gillespie.[24] The interference of the first- and second-order terms was assumed to be negligible.[25]

The events so generated were traced through the apparatus with a Monte Carlo simulation program which accounted for energy loss, multiple scattering, and the finite resolution of the detector. Thus, the yield and distributions of predicted events were obtained as well as the acceptance in any of the kinematic variables. Because of the requirement that all three muons have $p > 1.8$ GeV/c only a subsample of all tridents is observed. Total and effective cross sections along with the predicted yield of events are listed and compared with the data in Table III.

In Fig. 6 we show the predicted and observed distribution of the vertex of the trimuon events in the lead-glass target. The Monte Carlo simula-

TABLE III. Trident cross sections (in nb per lead nucleus) and yields.

	No exchange	Fermion	Observed
σ_{tot}, first Born approximation	739 ± 69	656 ± 67	
σ_{tot} with higher-order corrections	650 ± 61	577 ± 59	
σ within acceptance	61.8 ± 5.8	34.6 ± 3.5	36.3 ± 3.2
Number of events	233 ± 22	131 ± 14	137 ± 12

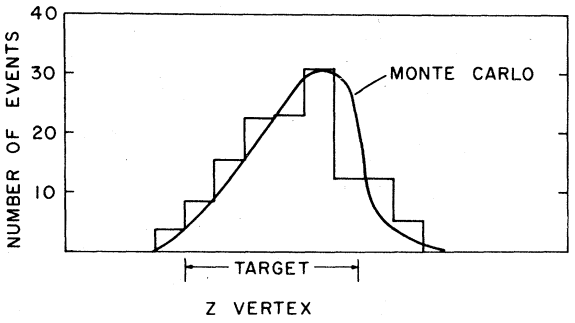

FIG. 6. The distribution of the vertex of trimuon events in the lead-glass target compared with the muon-trident Monte Carlo prediction.

tion predicts a vertex resolution of ±10 cm along the Z (beam) axis, in good agreement with the data.

The results of the QED and Monte Carlo calculations are compared with the data in Figs. 7–12. The solid curves show the cross section for events where all three muons have $p>1.8$ GeV/c and are

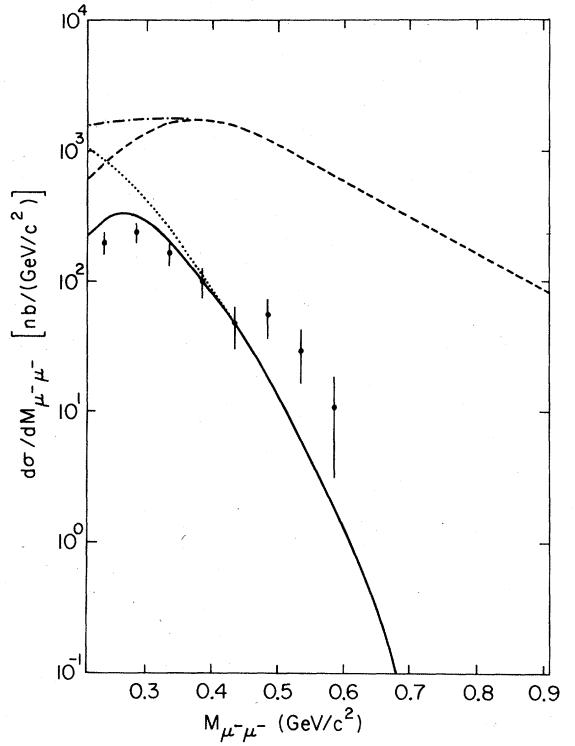

FIG. 7. The differential cross section in the effective mass of the two like-charge muons. Here, and in the following figures, the solid curve is the trident prediction for Fermi-Dirac muons with a momentum cut $p>1.8$ GeV/c, the dotted curve for muons with no exchange, and the dashed curve the QED prediction with no momentum cut. The dot-dash extension refers to no exchange and no momentum cut.

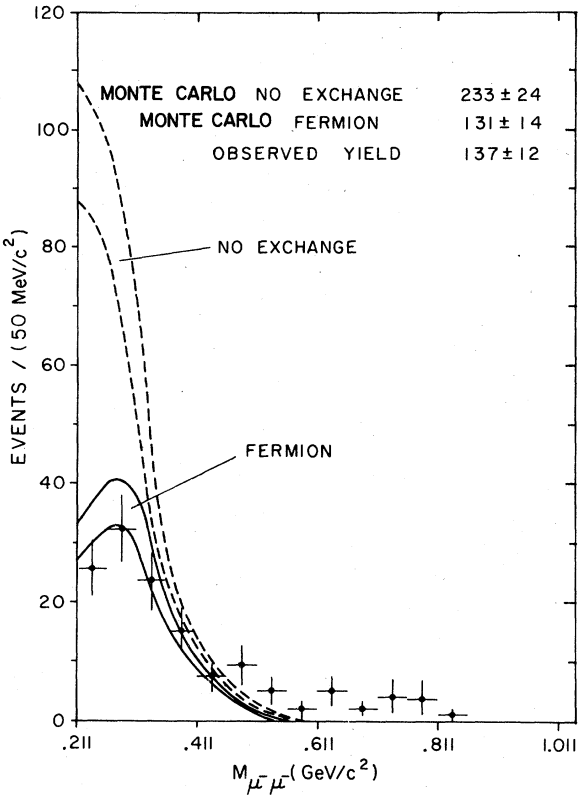

FIG. 8. The number of observed events as a function of $M_{\mu^-\mu^-}$ illustrating the effect of fermion exchange in the trident process.

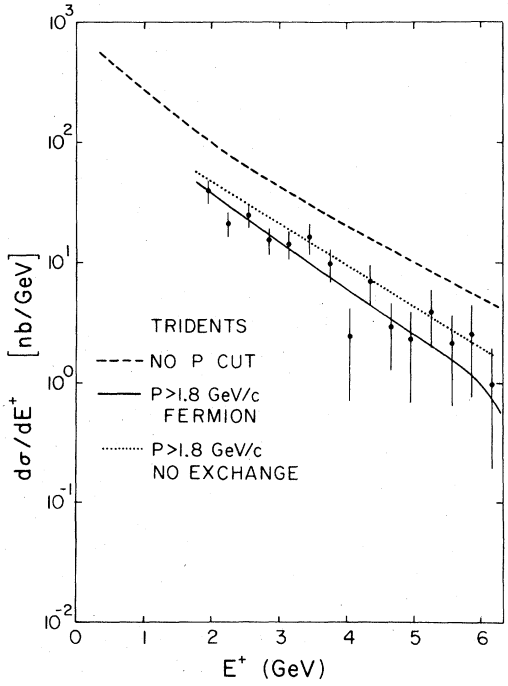

FIG. 9. The differential cross section in the energy of the positive (nonbeamlike) muon.

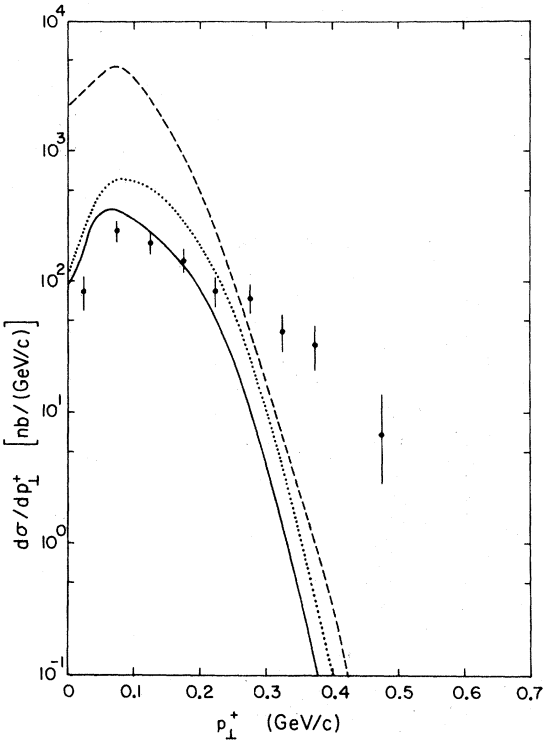

FIG. 10. The differential cross section in the transverse momentum of the positive muon.

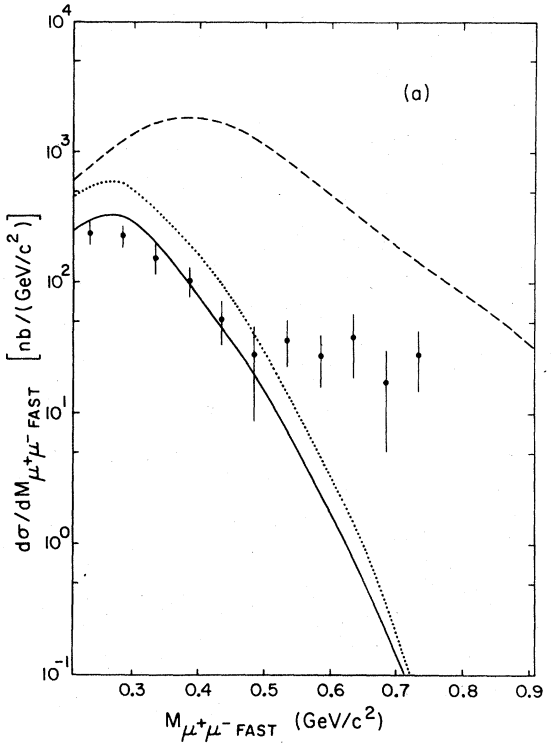

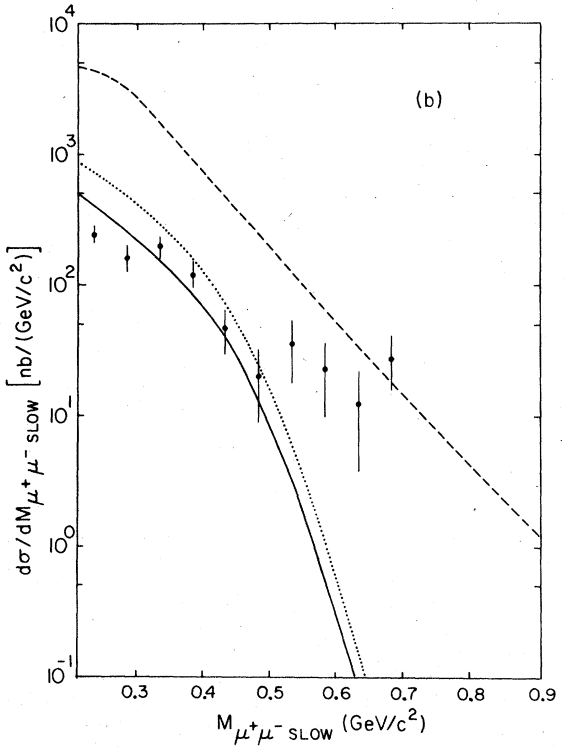

FIG. 11. The differential cross section in the effective masses of the $\mu^+\mu^-$ pairs where in (a) we have used the fast μ^- and in (b) the slow μ^-.

to be compared with the data points, which represent the observed events corrected for acceptance. The dotted curves show the same cross section under the assumption of no exchange for muons. Finally, for completeness, the dashed curves represent the total production cross section (i.e., when no restriction is placed on the muon momenta). We note that the normalization for both the data and theoretical curves has not been adjusted in anyway.

Figure 7 displays $d\sigma/dM$ for the effective mass of the like-charge muon pair $M_{\mu^-\mu^-}$. It is here that the effects of fermion exchange are most clearly seen as discussed in Sec. I. This data represents the second observation of this low-mass suppression attributed to the Pauli principle.[6] The effect is further illustrated in Fig. 8 where we show the number of observed events (after all corrections are applied) as a function of $M_{\mu^-\mu^-}$. The two bands give the prediction for fermions and for no exchange, respectively, the bandwidths indicating the uncertainty in the Monte Carlo integration of the cross section. The fermion assumption is strongly favored. Following the authors of Refs. 6 and 25 we define a parameter α such that

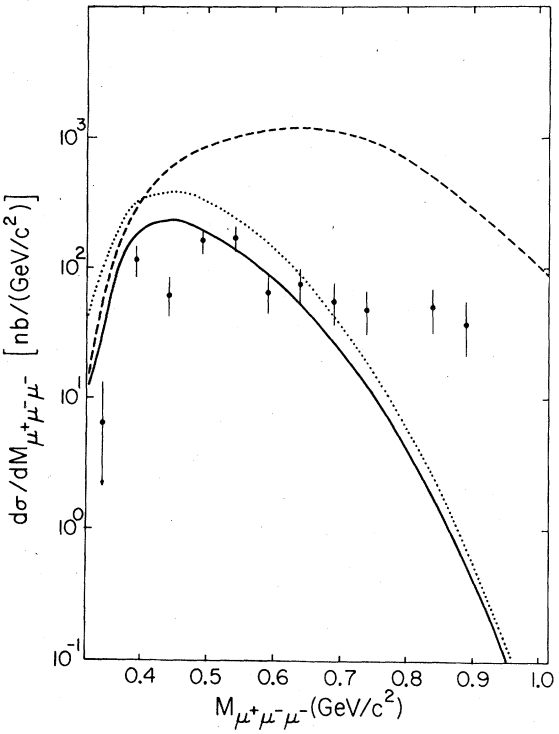

FIG. 12. The differential cross section in the three-muon effective mass.

$$\left(\frac{d\sigma}{dM_{\mu^-\mu^-}}\right)_{\text{meas}} = \left(\frac{d\sigma}{dM_{\mu^-\mu^-}}\right)_{\text{no ex}} + \alpha\left[\left(\frac{d\sigma}{dM_{\mu^-\mu^-}}\right)_{\text{ferm}} - \left(\frac{d\sigma}{dM_{\mu^-\mu^-}}\right)_{\text{no ex}}\right]. \quad (4)$$

Hence $\alpha = 1$ for fermions and $\alpha = 0$ for no exchange. A bin-by-bin maximum-likelihood fit to α yields

$$\alpha = 1.08 \pm 0.13, \quad (5)$$

where the error quoted combines both the fitting and Monte Carlo errors. The absence of the exchange effect would thus constitute an 8σ deviation from the data. We note that the effect arises primarily from the bins of lowest effective mass where the relative acceptance (i.e., for $p > 1.8$ GeV/c) is very good (~60%) and smoothly varying.

In Fig. 9 we show the differential cross section in the energy $E+$ of the produced positive muon. It is in excellent agreement in both normalization and shape with the QED trident prediction. We take this to be a further indication that the majority of trimuon events are indeed produced through this mechanism. Figure 10 shows $d\sigma/dp_\perp^+$ where $p_\perp^+$ is the transverse momentum of the μ^+. While the agreement here is good, a small excess of high-$p_\perp$ events is clearly evident. In Figs. 11(a) and 11(b) we show the effective-mass spectrum

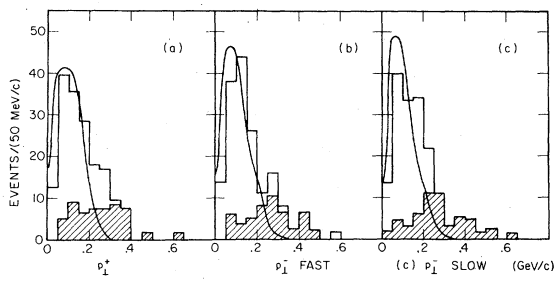

FIG. 13. The event distributions in the transverse momentum for (a) the positive final-state muon, (b) the fast negative muon, and (c) the slow negative muon. Curves shown are the Monte Carlo predictions for QED tridents. Shaded events represent $M_{3\mu} > 700$ MeV/c^2.

for the two $\mu^+\mu^-$ pairs where we have used the fast and slow μ^-, respectively, and in Fig. 12 the differential cross section in the three-muon mass. Most of the data is clustered at low mass and is accounted for by the trident hypothesis, yet we see a number of uncharacteristically high-mass events. We discuss these events below.

B. Elastic events; non-QED

In Fig. 10 we note an excess of events with at least one track at larger $p_\perp$ than is expected from QED tridents.[26] This excess is reflected in most of the distributions, in particular $M_{\mu^+\mu^-}$ (Fig. 11) and $M_{3\mu}$ (Fig. 12). To investigate these relatively wide-angle events, we look at events with $M_{3\mu} > 700$ MeV/c^2, while retaining the elasticity cut $|\Delta E| < 1.5$ GeV (Fig. 5). In Figs. 13(a)–13(c) the event distributions in the transverse momentum of the final state μ^+, fast μ^-, and slow μ^- are shown. Solid curves represent the Monte Carlo prediction for muon tridents, while shaded events indicate large three-muon mass. Clearly, the pure QED process cannot account for the entire set of elastic trimuons.

The most probable trimuon process that could possess this property is the vector-meson production mechanism of Fig. 3(a), where larger transverse momentum is expected from the decay of more massive particles. In Figs. 14(a) and 14(b) we show the effective-mass distribution of the two $\mu^+\mu^-$ combinations. No distinct peak is observed at the ρ^0 meson mass. This is not surprising in view of the small branching ratio of the ρ^0 into $\mu^+\mu^-$ (0.007%). However, investigation of the 13 events with one $\mu^+\mu^-$ pair having $700 < M_{\mu\mu} < 850$ MeV/c^2 reveals that the other $\mu^+\mu^-$ combination has mass $M_{\mu\mu} < 700$ MeV/c^2.

ρ^0 production by spacelike virtual photons has been measured in several experiments.[9,27] To compare our data with these results, we have taken the virtual-photon flux factor[28] correspond-

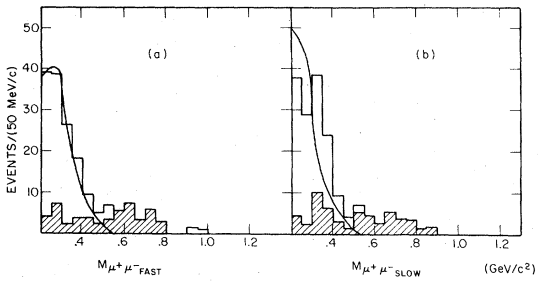

FIG. 14. The event distributions in the $\mu^+\mu^-$ mass for trimuons where we have used (a) the fast μ^- and (b) the slow μ^-. Curves are the Monte Carlo prediction for QED tridents.

ing to the Q^2 and ν of each ρ^0 candidate, the experimental acceptance, and the $\rho^0 \to \mu\mu$ branching ratio to extract the cross section $\sigma(\gamma_v + \mathrm{Pb} \to \rho^0 + \mathrm{Pb})$. The result, assuming an $A^{1.0}$ dependence,[29] is shown in Fig. 15, where it is seen to be consistent with the results of Ref. 27. We conclude that the non-QED excess of trimuons is almost entirely due to this known process.

C. Complete trimuon sample

Finally, we have investigated the set of 158 events in the entire trimuon sample (i.e., including events outside the ΔE cut). The three-muon mass distribution is shown in Fig. 16. No enhancements are evident, as might be expected from the exotic processes of Ref. 16 or a μ^* state of Fig. 3(d). In order to establish a limit on the production of such states, we have taken the excess yield over the trident process (including that accounted for in Sec. III B) to establish a maximum $B\sigma$ at the 90% confidence level. Using the acceptance for tridents at the same mass values, accounting for the three-muon mass resolution (± 70 MeV/c^2), and assuming an incoherent process we find

$$B\sigma < 7.0 \text{ (pb/nucleon)/(100 MeV/}c^2\text{)}$$

on the average over the range $500 < M_{3\mu} < 1400$ MeV/c^2.

The search for inelastic μ-pair production such as predicted by the graph of Fig. 3(b) is impaired by the lack of available phase space accessible in this experiment.[20] We observe 6 events with $\Delta E > 1.5$ GeV. Of these six events only one showed large energy deposition in the lead-glass target. We therefore assign 1^{+5}_{-1} events to this process and obtain a cross section per nucleon of

$$\sigma = 3.6^{+14.6}_{-3.6} \text{ pb/nucleon}$$

for the inelastic virtual Compton scattering process when the energy transferred to the hadrons exceeds 1.5 GeV. An extrapolation to our energy of the calculation of Ref. 11 yields an estimate for this process of $\sigma_T \sim 5$ pb/nucleon, in reasonable agreement with our result, which corresponds to an upper limit.

Alternatively, we can use the equivalent-photon approximation[28] to give an estimate for the inelastic Compton scattering cross section for quasi-real photons. The mean values of Q^2 and ν for

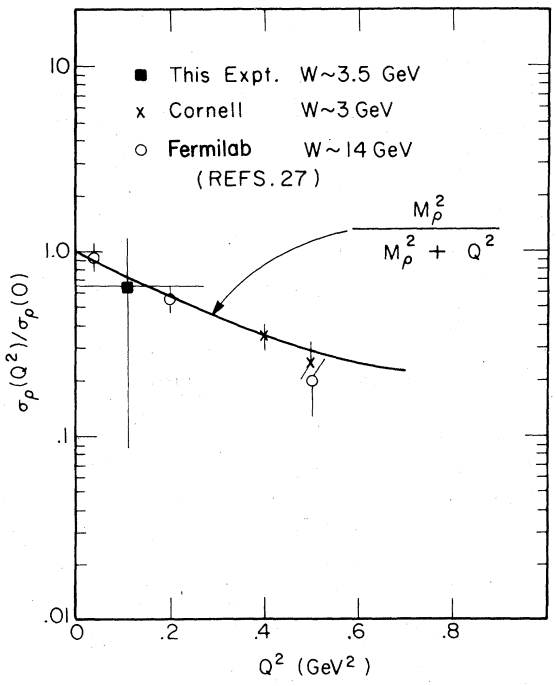

FIG. 15. The cross section for diffractive ρ production by virtual photons shown as a fraction of the ρ-photoproduction cross section. The square datum is the result of this experiment when an $A^{1.0}$ dependence is assumed. Other data are from Ref. 27.

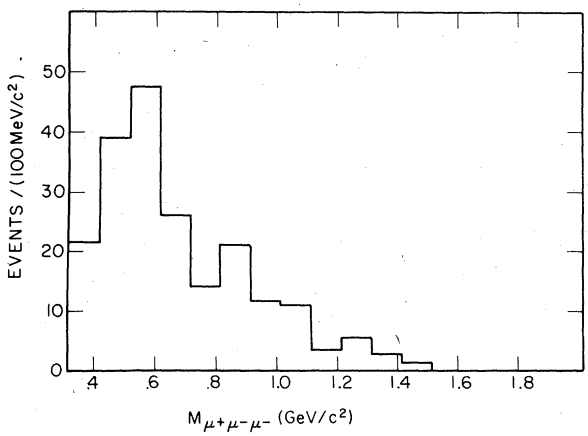

FIG. 16. The event distribution in the three-muon mass for all trimuon events.

these events are $\langle Q^2 \rangle = 0.03$ GeV^2 and $\langle \nu \rangle = 8.7$ GeV where Q^2 is the square of the four-momentum transfer of the leading particle to the target and ν the energy loss. Dividing by the virtual-photon flux factor we obtain

$$\sigma(\gamma_v N \to \mu^+\mu^- + X) \simeq 0.30^{+0.50}_{-0.09} \text{ nb/nucleon}.$$

While this result is based on very few events, we note that it disagrees with the significant excess of non-QED muon-pair events reported in Ref. 13. (We estimate that for this experiment we would observe a cross section of 6.5 nb/proton for Bethe-Heitler production of $\mu^+\mu^-$ by virtual photons on a *proton* target.)

IV. DIMUON EVENTS

In addition to the trimuon events described in Sec. III, 450 $\mu^+\mu^-$ and 223 $\mu^-\mu^-$ events were observed. It is clear from the calculation of the Bethe-Heitler graphs that in many cases of trident production one of the three muons will not have sufficient energy to be recorded in the apparatus leading to the detection of a dimuon final state. Furthermore, the muon-induced production of a hadronic final state with the subsequent decay of a meson into a muon also leads to a dimuon event.

In Figs. 17(a) and 17(b) we show the missing energy $\Delta E = E_{in} - E_{\mu_1} - E_{\mu_2}$ for both the $\mu^+\mu^-$ and $\mu^-\mu^-$ events. The events near $\Delta E = 0$ correspond to asymmetric tridents where the undetected muon has very low energy. The dashed curves give the predicted contribution from trident production.

To estimate the number of dimuon events from meson decay we have performed a Monte Carlo calculation. We use the virtual-photon spectrum[29] and the total photon-hadron cross section to obtain the number of hadronic events. The partial cross sections for inclusive $\pi^\pm$ and $K^\pm$ production were taken from SLAC (Ref. 30) and Cornell (Ref. 31) electroproduction data. The momentum distribution of the mesons in the photon-nucleon center-of-mass frame is assumed uniform whereas the angular distribution with respect to the virtual photon is taken to be of the form $e^{-4.5\theta}$ (an approximate parametrization of the data of Ref. 31). The mesons are required to emerge from the target and decay in flight in the region between the target and muon filter. The estimated yield is shown by the dotted curve in Figs. 17 and the total yield of dimuons by the solid curve. Table IV summarizes the results of the trident and meson-decay calculations and compares this with the observed dimuon yield for different cuts in ΔE.

The agreement between the calculations and the data is considered excellent in view of the uncertainties inherent in such calculations and because

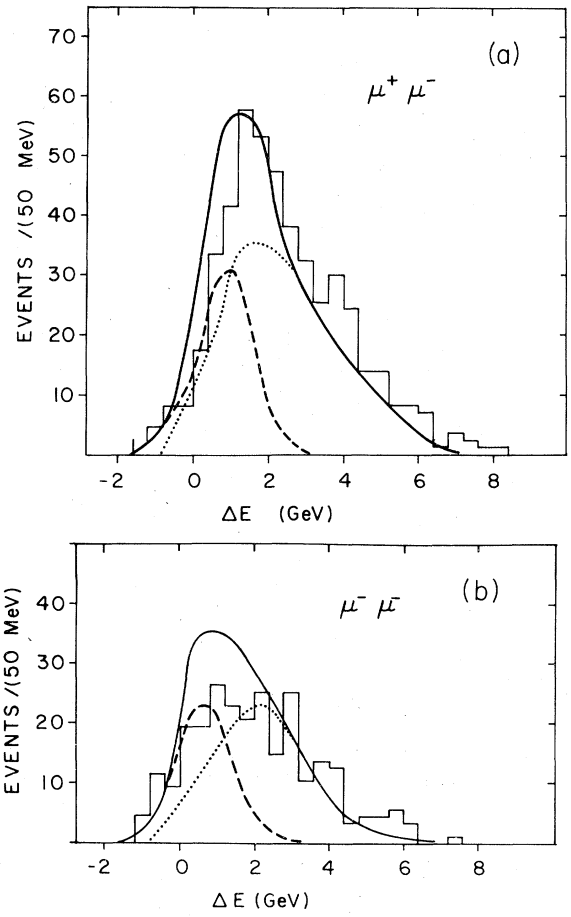

FIG. 17. The missing-energy distributions of dimuon events corrected for acceptance. Dashed curves are the calculated QED contribution and dotted curves the calculated meson-decay distribution. Solid curves are the total dimuon yield expected from these processes. (a) $\mu^+\mu^-$ pairs (b) $\mu^-\mu^-$ pairs.

the calculations have *not* been normalized to the data in any way. Furthermore, the agreement persists when any other distribution is tested including the scatterplot of E_- vs E_+ in the case of the $\mu^+\mu^-$ sample.[32] As a further example we show in Figs. 18(a) and 18(b) the effective-mass spectrum $M_{\mu^+\mu^-}$ and $M_{\mu^-\mu^-}$ for both dimuon samples together with the predicted yields. Again, the agreement is very good.

We conclude that even if genuine single-prompt-muon events occur, it is not possible to separate them in the presence of the dominant-trident and meson-decay backgrounds. Within our restricted range of available c.m. energy ($W < 4.5$ GeV) such a process could occur, for example, via the production of a neutral-heavy lepton which carries the muon quantum number[33]

TABLE IV. Predicted and observed dimuon events.

	$\mu^+\mu^-$	$\mu^-\mu^-$
	$\Delta E > -1$ GeV	
Monte Carlo		
Trident production	143 ± 15	118 ± 12
π decay	153 ± 20	131 ± 20
K decay	168 ± 26	59 ± 21
Totals	464 ± 36	308 ± 31
Observed	476 ± 23	256 ± 17
	$\Delta E > +2$ GeV	
Monte Carlo		
Trident production	7 ± 1	5 ± 1
π decay	83 ± 10	71 ± 10
K decay	117 ± 17	32 ± 11
Total	207 ± 20	108 ± 15
Observed	256 ± 17	125 ± 12

$$\mu^- + p \to M^0 + n$$
$$\searrow$$
$$\mu^+\mu^-\nu .$$

Since M^0 production would only show up in the $\mu^+\mu^-$ sample, we have considered the ratios

$$R = \left(\frac{\mu^+\mu^-}{\mu^-\mu^-}\right)_{\text{observed}},$$
$$= \frac{(\mu^+\mu^-)_{\text{trident}} + (\mu^+\mu^-)_{\text{meson decay}} + (\mu^+\mu^-)_{M^0}}{(\mu^-\mu^-)_{\text{trident}} + (\mu^-\mu^-)_{\text{meson decay}}} .$$

From this we find at the 90% confidence level that $N_{M^0} < 44$ events. Monte Carlo calculation estimates the acceptance for the $\mu^+\mu^-$ decay of a neutral heavy particle to be 0.20 ± 0.03 yielding

$$B\sigma(\mu^- N \to M_0 X) < 120 \text{ pb/nucleon}$$

assuming an $A^{1.0}$ dependence.

More generally, a single prompt muon could arise from the decay of a charged heavy lepton through

$$\mu^- N \to M^\pm \mu^- x$$
$$\searrow$$
$$\mu^\pm \nu .$$

Hence, we assume in the Monte Carlo calculations that such a particle is produced along the direction of the virtual photon, and estimate the acceptance for a dimuon final state to be 0.20 ± 0.03 and 0.16 ± 0.02 for the $\mu^+\mu^-$ and $\mu^-\mu^-$ events, respectively. Translating the excess of observed dimuons over predicted events (see Table IV) into 90% CL we obtain $N(\mu^+) < 59$ events and $N(\mu^-) < 24$ events. Hence

$$B\sigma(M^+) < 160 \text{ pb/nucleon},$$

$$B\sigma(M^-) < 80 \text{ pb/nucleon},$$

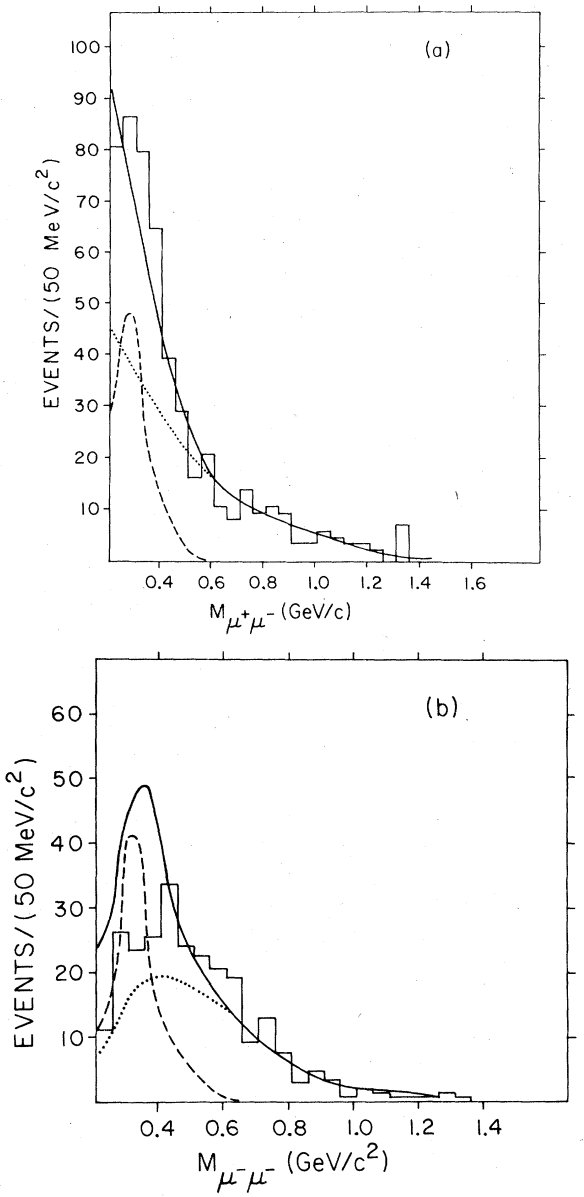

FIG. 18. Invariant-mass distributions for all observed pairs. (a) $\mu^+\mu^-$ pairs, (b) $\mu^-\mu^-$ pairs. Events are acceptance-corrected and curves correspond to those in Fig. 17.

again assuming an $A^{1.0}$ dependence. We note that the dimuon data agree well with the trident and meson-decay Monte Carlo predictions in all respects, including transverse-momentum distributions.

V. CONCLUSION

In summary, we have studied the characteristics of one and two-muon production by 10.5-GeV/c μ^- on a heavy nuclear target. The most prevalent

source of trimuons is the QED trident process. The observed trident distributions are in excellent agreement with predictions of the theory in both shape and total cross section. We have shown that muons exhibit exchange interference at a confidence level of 8 standard deviations. About 10% of the trimuons are uncharacteristic of the trident process and we attribute this to the strong diffraction of virtual photons. At higher energies this would imply characteristic peaks above the continuum production at the masses of the vector mesons as predicted by vector-meson dominance.[8,34] We have searched for enhancements in the three-muon mass spectrum and observe no such effect at a level of ~10 pb/nucleon with 90% confidence. Inelastic virtual-photon Compton scattering has recently been predicted[11] to be just within the range of our sensitivity, and indeed we observe a few possible inelastic trimuon events. Finally, the study of dimuon production shows (at the ~100 pb/nucleon level) that single-prompt-muon production at these energies can be fully accounted for by the two conventional processes of trident production and meson decay.

ACKNOWLEDGMENTS

We are indebted to many persons who made this experiment possible. We thank Dr. R. Rau, Dr. N. Samios, Dr. R. Palmer, Dr. H. Foelsche, and the staff of the AGS for their continuing support; Dr. H. Brown for the design of the beam and Professor S. L. Olsen for assistance in detector development. B. Wormington was essential to the design and construction of the apparatus, and we thank Dr. L. Leipuner for use of equipment from his group. J. Sanders, M. Van Lith, E. Frantz, R. Hogue, D. McCumber, and M. Austin provided excellent assistance during the various phases of the experiment. We are indebted to Dr. M. Tannenbaum for the use of his trident program. This work was supported in part by the U.S. Department of Energy.

---

*Present address: University of Wisconsin, Madison, Wisconsin 53706.
†Present address: Louisiana State University, Baton Rouge, Louisiana 70803.
‡Present address: LeCroy Research Systems, Spring Valley, New York 10977.
§Present address: Bell Laboratories, Murray Hill, New Jersey 07974.
‖Permanent address: York College of the CUNY, Jamaica, New York 11364.
¶Present address: University of Oklahoma, Norman, Oklahoma 73019.

[1]J. LeBritton *et al.*, Phys. Lett. 89B, 271 (1980).
[2]S. Brodsky and S. Ting, Phys. Rev. 145, 1018 (1966); J. Bjorken and M. Chen, *ibid.* 154, 1335 (1967); G. Reading Henry, *ibid.* 154, 1534 (1967); G. Homma *et al.*, J. Phys. Soc. Jap. 36, 1230 (1974).
[3]M. Tannenbaum, Phys. Rev. 167, 1308 (1968).
[4]L. Criegee *et al.*, Z. Phys. 158, 433 (1960).
[5]M. Morris and R. Stenerson, Nuovo Cimento 53B, 494 (1968); J. Barton and L. Rogers, *Proceedings of the Eleventh International Conference on Cosmic Rays, Budapest, 1969,* edited by T. Gemesv *et al.* (Akademia Kiaelo, Budapest, 1970), Vol. 4.
[6]J. Russell *et al.*, Phys. Rev. Lett. 26, 46 (1971).
[7]G. Grammer and J. Sullivan, in *Electromagnetic Interactions of Hadrons*, edited by A. Donnachie and G. Shaw (Plenum, New York, 1978), Vol. 2.
[8]H. Traas and D. Schildknecht, Nucl. Phys. B14, 543 (1969).
[9]J. Ballam *et al.*, Phys. Rev. D 5, 545 (1972); 7, 3150 (1973).
[10]CERN/European Muon Collaboration (private communication).
[11]V. Ganapathi and J. Smith, Phys. Rev. D 19, 801 (1979).
[12]See, for instance, H. Jöstlein *et al.*, Phys. Lett. 52B, 485 (1974).
[13]J. Davis *et al.*, Phys. Rev. Lett. 19, 1356 (1972).
[14]D. Caldwell *et al.*, Phys. Rev. Lett. 33, 868 (1974).
[15]H. Primakoff, Phys. Rev. 81, 899 (1951).
[16]J. Pati and A. Salam, Phys. Rev. Lett. 31, 661 (1973); Phys. Rev. D 10, 275 (1975).
[17]C. Chang *et al.*, Phys. Rev. Lett. 39, 519 (1977).
[18]A. Entenberg *et al.*, Phys. Rev. Lett. 32, 486 (1974).
[19]H. Brown (private communication).
[20]For a muon to be detected under these circumstances it must have energy $E > 3.2$ GeV, which leaves only ~1 GeV of additional energy to be shared between the three muons (on the average ~0.3 GeV to exit the target, ~1 GeV to traverse the brass absorber, and ~1.9 GeV to penetrate the rear filter).
[21]Y. Tsai, Rev. Mod. Phys. 46, 815 (1974).
[22]By "no exchange" we mean that in calculating the Feynman diagrams of Fig. 1 the two final-state μ^- are treated as nonidentical fermions. Thus there is no need to include the four exchange amplitudes (in which p_2 and p_4 are interchanged) nor is there a need for a statistical factor of 1/(2!). The net result is that the "fermion cross section" includes the interference of normal and exchange amplitudes while the "no-exchange cross section" does not. In effect, it is this interference that we are measuring. For more details, see Ref. 3.
[23]H. Bethe and L. Maximon, Phys. Rev. 93, 768 (1954).
[24]S. Brodsky and J. Gillespie, Phys. Rev. 173, 1011 (1968).
[25]Based on the expression for the interference of one-

and two-photon-exchange amplitudes for muon-pair photoproduction given in Ref. 23, we estimate this term to be a correction of at most a few percent. However, the two-photon-exchange diagrams for the trident process have not been calculated. See R. Sah, Harvard University thesis, 1970 (unpublished).

[26]The trident cross section is overwhelmingly dominated by the region where each final-state muon has $p_T \lesssim 2m_\mu$ as can be seen in Fig. 13. See Ref. 3.

[27]J. Ballam *et al.*, Phys. Rev. D 10, 765 (1974); L. Ahrens *et al.*, Phys. Rev. Lett. 42, 208 (1979); 31, 131 (1973); W. Francis, *et al.*, *ibid.* 38, 633 (1977).

[28]H. Terazawa, Rev. Mod. Phys. 45, 615 (1973).

[29]The average mass of these events is $\langle M \rangle = 766$ MeV/c^2 with full width $(2\sigma) = 135$ MeV/c^2. We used $\sigma(\gamma p \to \rho p) = 18.5$ μb.

[30]J. Martin *et al.*, Phys. Lett. 65B, 483 (1976).

[31]C. Bebek *et al.*, Phys. Rev. D 15, 3085 (1977); 15, 594 (1977); E. Lazarus *et al.*, Phys. Rev. Lett. 29, 743 (1972).

[32]Correlations between the energies of the two muons occur when the dimuon results from the muonic decay of a heavy particle. See Ref. 17.

[33]J. Bjorken and C. Llewellyn Smith, Phys. Rev. D 7, 887 (1973).

[34]J. J. Aubert *et al.*, Phys. Lett. 89B, 267 (1980).